

Design of a multi-material acoustic black hole

Beth Austin¹, Jordan Cheer² Institute of Sound and Vibration Research University of Southampton University Road, Southampton, SO17 1BJ

Anil Bastola³ Centre for Additive Manufacturing University of Nottingham Nottingham, NG7 2RD

ABSTRACT

Acoustic black holes (ABHs) have been proven as an effective passive vibration control measure. Typically, they are realised by introducing a geometric taper into a structure. This approach introduces thin structural sections which leaves the ABH prone to damage through mechanisms such as static failure or fatigue. An alternative approach has been suggested in which the material properties vary within the structure, which can be realised through multi-material additive manufacturing. This allows the structure to maintain a constant thickness and this may reduce the effect of fatigue. Prior work has been performed to characterise the materials currently available that would be suitable for the ABH application. This paper investigates methods of optimising the design of the multi-material ABH, in order to minimise the reflection coefficient in a beam termination application.

1. INTRODUCTION

The concept of an ABH has been around for many years. The base theory was first suggested by Mironov in 1988 [1] before being adapted into what is now referred to as an acoustic black hole by Krylov in 2004 [2]. Since then, the development of so called geometric ABHs has continued, with further study into their potential applications and capabilities [3]. One major benefit of the geometric ABH is that the structural vibration decrease is brought about without adding additional material and hence mass to the structure and thus provides an inherently lightweight vibration control treatment.

One noteworthy issue that all geometric ABHs encounter is the reduced strength of the structure due to the tapering thickness required to reduce the wavespeed and achieve characteristic ABH behaviour. This leaves the structure susceptible to damage through both impact and fatigue from

¹eha1g17@soton.ac.uk

²j.cheer@soton.ac.uk

³Anil.Bastola@nottingham.ac.uk

the repeated loading of the structure. However, it is also possible to achieve a decrease in the wavespeed through changing the material properties along the length of the ABH rather than the external geometry. A variety of methods have been proposed to introduce this variation including changing material porosity [4], application of thermal gradients [5], and grading materials through multi-material additive manufacturing [6]. Alternatively, to avoid the need for a continuously varying material profile, discrete sections of materials may be used to closely approximate the desired gradient in what is known as a multi-material ABH. In this paper, a method of optimising the section lengths required to achieve optimal performance from a multi-material ABH is proposed and its performance is investigated via numerical simulations.

An initial investigation into graded material properties that could be realised through additive manufacturing was presented in [6]. However, the first order WKB approximation [1,2] was used in the presented analysis, which does not account for reflection from the junction between the beam and taper or at material boundaries that will occur in the proposed multi-material design. Moreover, investigations in [6] did not consider the effect of a varying loss factor for each material. This previous analysis may, therefore, suggest better performance than is actually achievable from the multi-material ABH. As such, further investigation is required to take into account the practical effects of realising a multi-material ABH. As such, this paper will present an investigation into the design and optimisation of a multi-material ABH beam termination using a finite element modelling approach. Section 2 describes the multi-material ABH design concept in relation to a conventional geometric ABH. Section 3 presents an investigation into the optimum material section lengths to provide broadband vibration attenuation.

2. ABH BEAM TERMINATIONS

2.1. Geometric ABH

Typically, an ABH is realised by varying the geometrical properties of the structure to cause a reduction in wave speed. In beams, the wave speed can be expressed in terms of geometrical and material properties as [2,7]

$$c_f(x) = \left(\frac{E(x)h(x)^2\omega^2}{12\rho(x)}\right)^{1/4}$$
 (1)

where c_f is the wave speed at a given frequency f, x is the coordinate position along the beam, E is the Young's modulus, h is the height of the structure, ω is the angular frequency, and ρ is the density. Equation 1 clearly shows that the wave speed is proportional to the square of the beam height. In a geometric ABH, the height typically follows a power law profile given by

$$h(x) = (h_0 - h_{tip}) \left(\frac{l_{ABH} - x}{l_{ABH}} \right)^{\mu} + h_{tip}$$
 (2)

where l_{ABH} is the length of the ABH section, x is the position along the taper, h_0 is the height of the unmodified beam, and h_{tip} is the height at the end of the taper. It should be noted that in Equation 1, x refers to the position along the total length of the beam whereas in Equation 2, x refers to the position along the ABH section only with position x = 0 being the junction between the uniform beam and the ABH taper.

The performance of an ABH beam termination is typically quantified by the reflection coefficient

and this can be calculated using [8]

$$|R| = \left| \frac{\Phi^-}{\Phi^+} \right| \tag{3}$$

where Φ^- and Φ^+ are the complex amplitudes of the negative and positive propagating waves in the beam respectively. The propagating wave amplitudes can be calculated in terms of the transverse velocity at two sensor points along the beam as follows:

$$\Phi^{+} = \frac{-1}{2\omega \sin(k\Delta)} \left(v(x_1)e^{jk\Delta/2} - v(x_2)e^{-jk\Delta/2} \right)$$
 (4)

$$\Phi^{-} = \frac{-1}{2\omega \sin(k\Delta)} \left(v(x_1)e^{-jk\Delta/2} + v(x_2)e^{jk\Delta/2} \right)$$
 (5)

where Δ is the distance between sensor points, x_1 and x_2 are the locations of each sensor on the beam, v is the transverse velocity at x, and k is the wave number at frequency ω . The wave number is defined as

$$k(x) = \frac{\omega}{c_f(x)} = \left(\frac{12\rho(x)\omega^2}{E(x)h(x)^2}\right)^{1/4}.$$
 (6)

In an ideal scenario, the beam would terminate with a tip height of zero. However, this is not possible due to the limitations of manufacturing methods. Instead, the wedge is truncated leaving the finite tip height, h_{tip} , thus preventing total dissipation of the wave energy and causing reflection of the wave back into the beam. To mitigate this, a layer of additional damping material is typically added to the surface of the ABH, as can be seen in Figure 1. This counteracts some of the influence of the necessary wedge truncation by allowing additional energy dissipation due to the higher loss factor of the damping material.

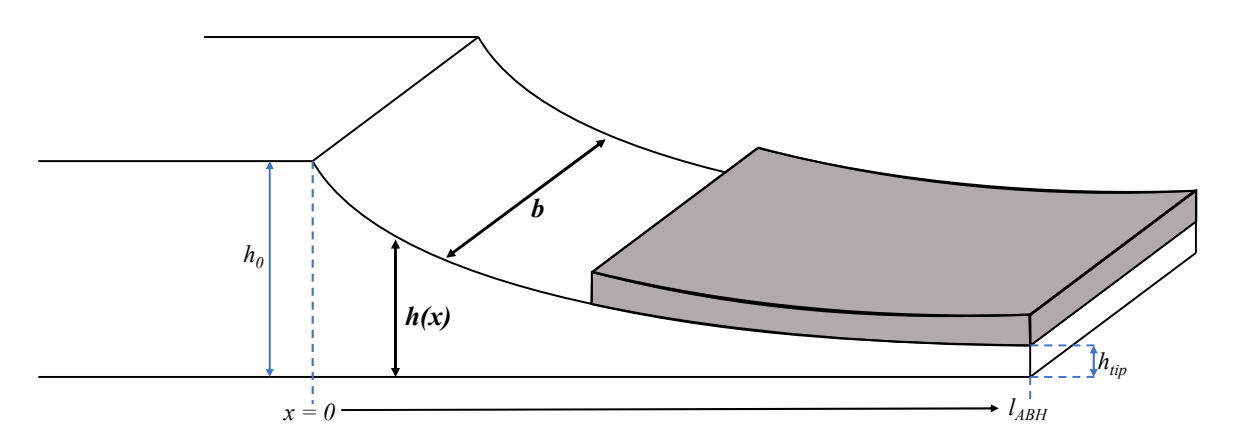


Figure 1: A geometric ABH with added damping layer

2.2. Graded Material ABH Material Properties

As suggested by Equation 3, an alternative means to obtain a decreasing wavespeed profile is to realise a structure with a decreasing Young's modulus. Theoretically, in order to match the behaviour of the geometric power law profile, the Young's modulus in the taper should follow the profile given as

$$E(x) = \left(\frac{h(x)^2}{h_0^2}\right) E_0 \tag{7}$$

where E_0 is the Young's modulus of the beam material. In this instance, x refers to position along the ABH section only and x = 0 occurs at the juction between the beam and ABH. Using Equations 2 and 7, it is possible to find the configuration of the graded Young's modulus ABH that matches

the geometric ABH performance as previously discussed in [6]. This would require a continuously variable Young's modulus and would also assume that damping remains constant as the Young's modulus is varied.

This multi-material ABH concept is shown graphically in 2 and in this scenario, the objective is to specify or optimise the section lengths for a pre-selected set of materials to minimise the reflection coefficient. For the purpose of this investigation, it has been assumed that a discrete set of 8 materials is available for the multi-material ABH design. These materials are based on a mix of the Stratasys Connex digital materials with the properties detailed in Table 1.

Material	VeroClear	RGD8710	RGD8720	RGD8730	FLX9095	FLX9070	FLX9050	Tango+
E(GPa)	2.347	2.068	1.905	1.589	0.0708	0.0046	0.0016	0.0006
η	0.0609	0.0677	0.0729	0.1154	0.4524	0.7386	0.9722	1.0512
$\rho(\text{kgm}^{-3})$				1160				

Table 1: Properties of the Stratasys Connex digital materials

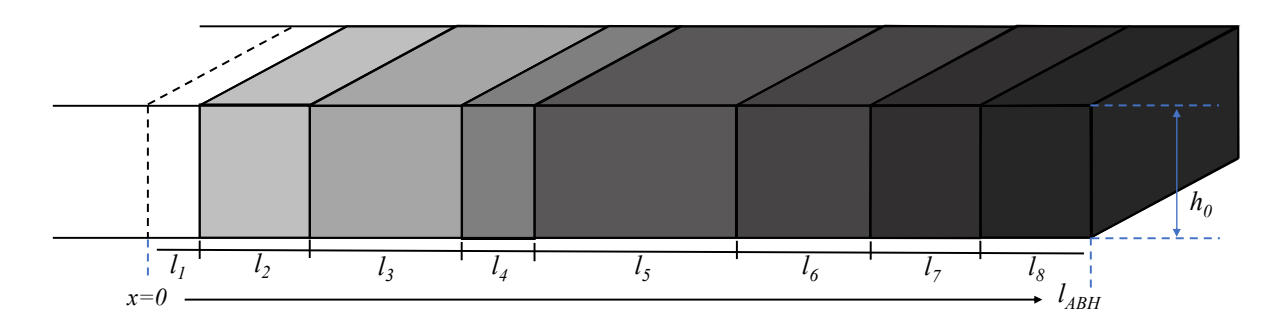


Figure 2: A multi-material ABH

Given the assumed range of materials defined in 1, it is possible to calculate the tip height for a geometric ABH with the corresponding range of effective Young's modulus by rearranging Equation 7. With the given range of materials, for a VeroClear beam of height $h_0 = 10$ mm, this gives the corresponding tip height as

$$h_{tip} = h_0 \sqrt{\frac{E_{Tango+}}{E_{VeroClear}}} = 0.16mm. \tag{8}$$

This tip height can be substituted into Equation 2 to find the taper height profile for such a geometric ABH. For this investigation, a power $\mu=4$ and length $l_{ABH}=7$ cm were used. This profile h(x) can then be substituted back into Equation 7 to find the variation in effective Young's modulus along the length of the ABH that best matches teh power law profile. The point at which the Young's modulus of each of the Stratasys materials best matches this profile can then be found. The material section lengths that correspond to these points are given in Table 2 and serve as a reference point against which the performance of the section length optimisation procedure, described in the following section, can be compared.

3. SECTION LENGTH OPTIMISATION

To investigate the performance of both a power law profile matched and an optimised multimaterial ABH, a COMSOL finite element model was implemented wherein a VeroClear beam is terminated by a multi-material ABH. For the optimisation starting point, the ABH consisted of equal, discrete lengths of each material in order of decreasing Young's modulus, starting with VeroClear and ending with Tango+. The optimisation problem was defined to minimise the average reflection coefficient across a frequency range 20Hz - 10kHz, with a constraing on the sum of the section lengths being equal to the total ABH length of 7cm. This constrained, non-linear optimisation problem was solved using the MATLAB multistart routine with the fmincon solver [9]. This optimisation procedure uses a gradient descent based algorithm and multiple start points, including the initial start point and 9 additional random start points, with the objective of finding a global minimum.

The material section lengths can be found in Table 2 for both the power law matched multi-material ABH and the optimised multi-material ABH. Overall, the section lengths are similar, however the optimised configuration does suggest an increase in the length of Tango+, which may be explained by the higher damping provided by this material. suggests the optimisation is maximising the damping properties of the structure. In addition, the optimised configuration increases the length of VeroClear, which effectively decreases the length of the ABH.

Material	VeroClear	RGD8010	RGD8020	RGD8030	FLX9095	FLX9070	FLX9050	Tango+
Geometric	0.0011	0.0007	0.0016	0.0223	0.0155	0.0067	0.0154	0.0067
Optimisation	0.0043	0.0007	0.0005	0.0220	0.0155	0.0083	0.0050	0.0127

Table 2: Material section lengths of an optimised multi-material ABH

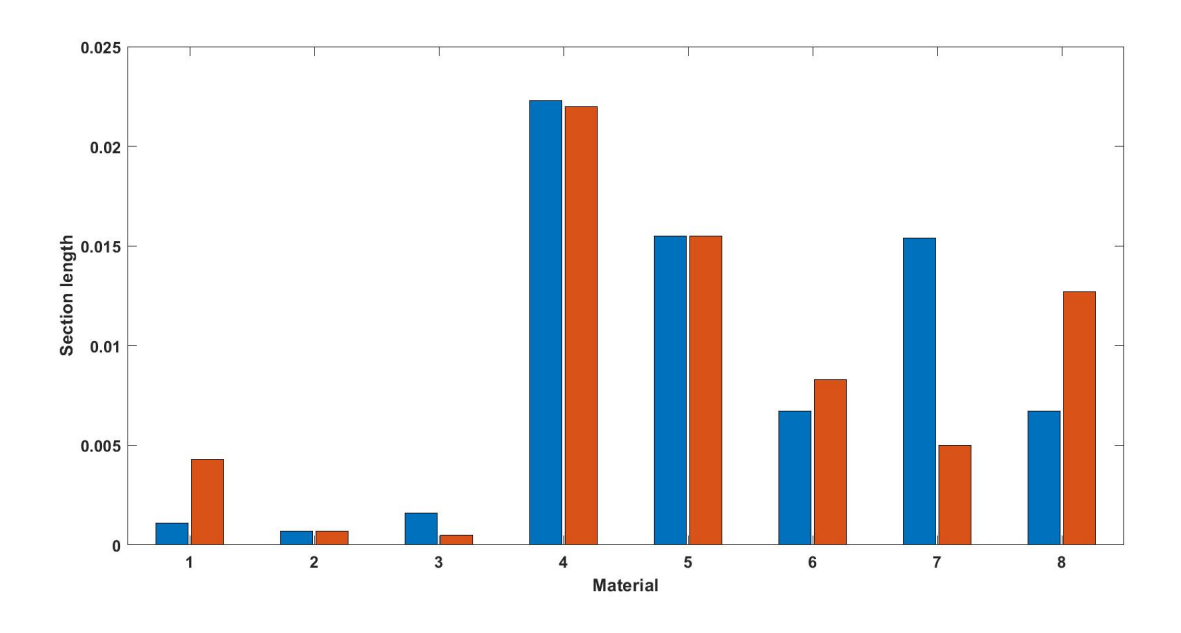


Figure 3: Material section lengths of a multi-material ABH for the geometric equivalent ABH in blue and the optimised ABH in red

A 2D COMSOL model of a geometric ABH was implemented to provide a comparison for the multi-material ABHs. This model consisted of a VeroClear beam with a geometric ABH termination with taper parameters $\mu = 4$, $l_{ABH} = 7$ cm, and $h_{tip} = 0.16$ mm. Geometric ABHs typically have a damping layer added to improve performance. As such, a uniform thickness Tango+ damping layer was applied over the top face of the taper as shown in 1. The layer thickness and length of the damping layer were set to 1.2mm and 6cm respectively, which maximises performance in line with [10].

The broadband average reflection coefficient of each ABH configuration discussed can be found in Table 3, along with the reflection coefficient of a VeroClear beam of constant thickness. All ABH

configurations provide a reduction in the reflection coefficient of at least 60% compared to a standard beam. This significant reduction in vibration reflection indicates that multi-material ABHs are a potential alternative to geometric ABHs.

Configuration	Uniform Beam	Power Law Matched	Optimised	Damped Geometric
$R_{average}$	0.5421	0.2125	0.2083	0.1950

Table 3: Broadband average reflection coefficients for a range of ABH beam termination configurations

To provide more detail, Figure 4 shows the reflection coefficient across frequencies for all configurations. From this plot it can be seen that the behaviour of the geometric ABHs differs significantly from that of the multi-material ABHs investigated. Performance of the multi-material ABHs surpass that of the geometric ABH at frequencies below 1kHz, despite the significant dips in the profile of the damped geometric ABH. However, the opposite is true at higher frequencies.

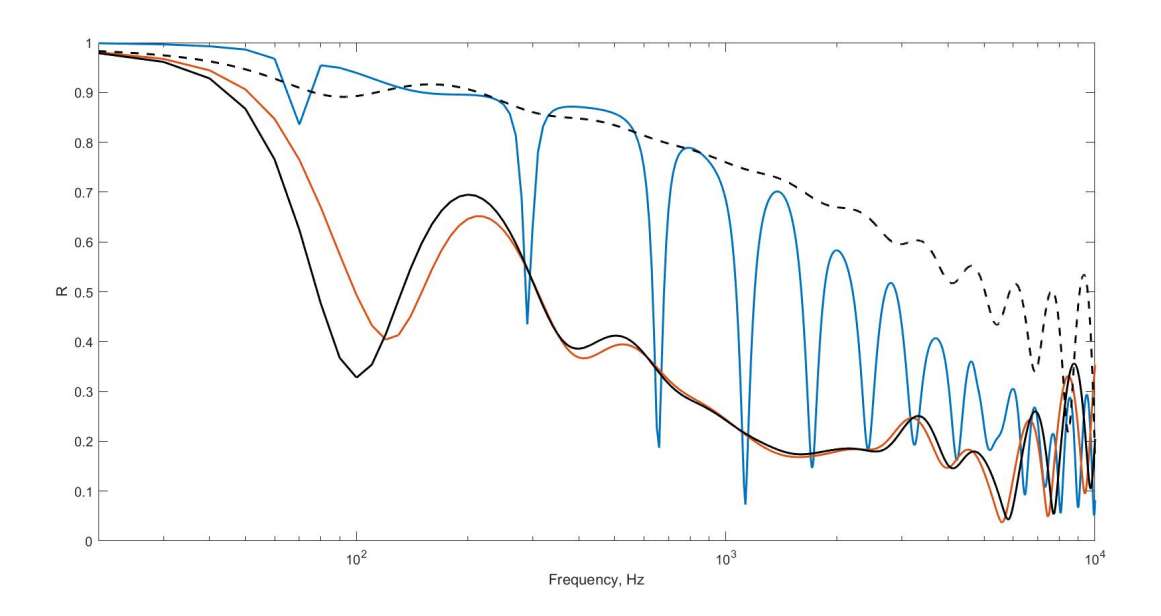


Figure 4: Reflection coefficient for various beam terminations: uniform beam (dashed black), geometric equivalent multi-material ABH (solid black), optimised multi-material ABH (solid red), geometric ABH with damping layer (solid blue).

There are some slight differences between the two multi-material ABHs investigated. There is a slight improvement in performance at higher frequencies in the optimised multi-material ABH compared to the geometrical equivalent multi-material ABH, which may be related to the decresed effective length of the ABH. There is, however, minimal difference between the two and the profiles of the two multi-material configurations are similar.

4. CONCLUSIONS

This paper has presented an initial investigation into the performance of multi-material ABHs. This builds on previous work by investigating the effect of a change in multiple material properties, namely Young's modulus and loss factor, along the length of a multi-material ABH. It has been demonstrated that the multi-material ABH could be a potential alternative to geometric ABHs, particularly in application where the thin tip of a geometric ABH is impractical. Further investigation is required to

experimentally validate these findings and to better understand the impact of each changing material parameter.

5. ACKNOWLEDGEMENTS

This work was supported by an EPSRC Prosperity Partnership (No. EP/S03661X/1). The authors acknowledge the use of the IRIDIS High Performance Computing Facility and associated support services at the University of Southampton in the completion of this work.

REFERENCES

- [1] M A Mironov. Propagation of a flexural wave in a plate whose thickness decreases smoothly to zero in a finite interval. *Soviet Physics Acoustics-Ussr*, 34(3):318–319, 1988.
- [2] V. V. Krylov and F. J.B.S. Tilman. Acoustic 'black holes' for flexural waves as effective vibration dampers. *Journal of Sound and Vibration*, 274:605–619, jul 2004.
- [3] Adrien Pelat, François Gautier, Stephen C. Conlon, and Fabio Semperlotti. The acoustic black hole: A review of theory and applications. *Journal of Sound and Vibration*, 476:115316, jun 2020.
- [4] Weiguang Zheng, Shiming He, Rongjiang Tang, and Shuilong He. Damping Enhancement Using Axially Functionally Graded Porous Structure Based on Acoustic Black Hole Effect. *Materials* 2019, Vol. 12, Page 2480, 12(15):2480, aug 2019.
- [5] Vasil Georgiev, Jacques Cuenca, Miguel Moleron Bermudez, François Gautier, and Laurent Simon. Recent progress in vibration reduction using Acoustic Black Hole effect. In 10ème Congrès Français d'Acoustique, 2010.
- [6] Jordan Cheer and Steve Daley. On the potential of a functionally graded acoustic black hole using multi-material additive manufacturing. In *Proceedings of 2020 International Congress on Noise Control Engineering, INTER-NOISE 2020*, 2020.
- [7] K. Hook, J. Cheer, and S. Daley. A parametric study of an acoustic black hole on a beam. *The Journal of the Acoustical Society of America*, 145(6):3488–3498, 2019.
- [8] C. R. Fuller, S. J. (Stephen J.) Elliott, and P. A. Nelson. *Active control of vibration*. Academic Press, 1996.
- [9] Richard H. Byrd, Jean Charles Gilbert, and Jorge Nocedal. A trust region method based on interior point techniques for nonlinear programming. *Mathematical Programming*, 89(1):149–185, 2000.
- [10] V. V. Krylov. New type of vibration dampers utilising the effect of acoustic 'black holes'. *Acta Acustica united with Acustica*, 90(5):830–837, 2004.